

Maximizing the DUNE early physics output with current experiments

Monojit Ghosh^{1,a}, Srubabati Goswami^{1,b}, Sushant K. Raut^{1,2,c} 

¹ Physical Research Laboratory, Navrangpura, Ahmedabad 380 009, India

² Department of Theoretical Physics, School of Engineering Sciences, KTH Royal Institute of Technology–AlbaNova University Center, Roslagstullsbacken 21, 106 91 Stockholm, Sweden

Received: 12 October 2015 / Accepted: 21 February 2016 / Published online: 2 March 2016
© The Author(s) 2016. This article is published with open access at Springerlink.com

Abstract The deep underground neutrino experiment (DUNE) is a proposed next generation superbeam experiment at Fermilab. Its aims include measuring the unknown neutrino oscillation parameters—the neutrino mass hierarchy, the octant of the mixing angle θ_{23} , and the CP-violating phase δ_{CP} . The current and upcoming experiments T2K, NO ν A, and ICAL@INO will also be collecting data for the same measurements. In this paper, we explore the sensitivity reach of DUNE in combination with these other experiments. We evaluate the least exposure required by DUNE to determine the above three unknown parameters with reasonable confidence. We find that for each case, the inclusion of data from T2K, NO ν A, and ICAL@INO help to achieve the same sensitivity with a reduced exposure from DUNE thereby helping to economize the configuration. Further, we quantify the effect of the proposed near detector on systematic errors and study the consequent improvement in sensitivity. We also examine the role played by the second oscillation cycle in furthering the physics reach of DUNE. Finally, we present an optimization study of the neutrino–antineutrino running of DUNE.

1 Introduction

The flavor mixing of neutrinos leading to neutrino oscillations was confirmed by the Super-Kamiokande experiment [1], more than a decade ago. In the years since, we have measured most of the neutrino oscillation parameters to some precision. Solar neutrino experiments like SNO [2,3] and the reactor neutrino experiment KamLAND [4] have measured the solar oscillation parameters θ_{12} and Δ_{21} ($=m_2^2 - m_1^2$)

quite precisely. The atmospheric parameters θ_{23} and $|\Delta_{31}|$ ($=|m_3^2 - m_1^2|$) have been measured by Super-Kamiokande, MINOS and T2K [5–7]. The smallest mixing angle θ_{13} has been measured quite recently by the reactor neutrino experiments Double Chooz, Daya Bay, and RENO [8–10]. The combined fit to world neutrino data significantly constrains most of the oscillation parameters today [11–13].

Some quantities, however, still remain unmeasured. The sign of the atmospheric mass-squared difference Δ_{31} is currently unknown. The case with $m_3 > m_1$ ($m_3 < m_1$) is called a normal (inverted) hierarchy or NH(IH). The octant in which the atmospheric mixing angle lies is another unknown. If $\theta_{23} < 45^\circ$ ($\theta_{23} > 45^\circ$), then θ_{23} is said to lie in the lower (higher) octant or LO(HO). Finally, the value of the CP-violating phase δ_{CP} is completely undetermined with the whole range from -180° to $+180^\circ$ being allowed at 3σ C.L. However, recent hints point to a value of δ_{CP} close to -90° [14]. There are many other fundamental questions, like the absolute masses of the neutrinos and their Dirac/Majorana nature. However, these cannot be probed by neutrino oscillation experiments.

The primary task before the current and next generation of neutrino oscillation experiments is therefore, to measure the unknown parameters (mass hierarchy, octant of θ_{23} , and δ_{CP}) and to put more precise constraints on the values of the known ones. These can be achieved by experiments that probe the $\nu_\mu \rightarrow \nu_e$ and $\nu_\mu \rightarrow \nu_\mu$ oscillation channels at scales relevant to the atmospheric mass-squared difference. The superbeam experiments T2K [15] and NO ν A [16] which are operational are the two current generation long-baseline experiments that are likely to shed light on the above issues. The discovery of a non-zero θ_{13} and a precise measurement of this parameter have added a boost to the explorations of the potential of these experiments toward measuring the above unknowns [17–28]. Some of the earlier studies on this topic can be found in [29–31]. Atmospheric neutrino experiments

^a e-mail: monojit@prl.res.in

^b e-mail: sruba@prl.res.in

^c e-mails: sushantkr@gmail.com; raut@kth.se

can also throw light on the above issues. One such project, ICAL@INO [32], is already approved and will use a magnetized iron calorimeter detector with charge sensitivity. The combined capabilities of the long-baseline experiments T2K, NO ν A, and the atmospheric neutrino experiment ICAL have been discussed extensively, e.g. see Refs. [22,23,26,33–35].

The main problem in determining the oscillation parameters is the problem of parameter degeneracy [36–41], i.e. two different sets of oscillation parameters giving the same value of probability. Therefore, in the degenerate parts of the parameter space, it is difficult for any one experiment to measure all the unknown parameters [42–47]. Depending on the values of the oscillation parameters in nature, the current and upcoming experiments may be able to measure one or more of the unknown parameters over the next few years. However, the expected sensitivity even in favorable parameter space is in the range $2\text{--}3\sigma$. For unfavorable values of parameters as well as for enhanced sensitivity in the favorable region we will need next generation facilities. The LBNE experiment [48] in the United States and the LBNO experiment [49] in Europe were two of the proposals for such a facility. Many studies have explored the physics reach of these experiments [28,50–61]. These different proposals are now converging into a unified endeavor of a long-baseline experiment using a high-intensity beam from Fermilab. The proposal outlines construction of a deep underground neutrino observatory at Sanford underground research facility (SURF) in South Dakota. This was initially called the Experiment at the Long Baseline Neutrino Facility (ELBNF) [62], now re-christened as DUNE. The prospective detector is a modular 40 kiloton liquid argon time projection chamber (LArTPC). One of the major goals of this facility as outlined in [63] is a 3σ CP sensitivity for 75 % values of δ_{CP} .

There are also proposals for future atmospheric neutrino experiments, such as HyperKamiokande [64,65] which is a Water Čerenkov detector and PINGU [66] which is a Multi-Megaton ice detector using the Čerenkov technique. Some phenomenological studies involving these experiments have been presented in Refs. [67–71].

By the time the next generation experiments start collecting data, we will also have information from the current generation of experiments NO ν A, T2K and the upcoming ICAL experiment. It is therefore pertinent to ask what the minimum amount of information needed from the future experiments in light of the information from this data is. This question was addressed in Ref. [54] in the context of the LBNO experiment. In that paper, three prospective baselines namely 2290, 1540, and 130 km were considered for the LBNO configuration. For the first two baselines the prototype detector was a LArTPC, whereas for the 130 km baseline a Čerenkov detector was considered. It was shown that there exists a synergy between experiments and channels, because

of which the combined analysis of many experiments gives very good sensitivity. Therefore the same physics goals can be achieved with a lower exposure for LBNO. In this work, we carry out a similar analysis for DUNE with a baseline of 1300 km and taking a LArTPC detector. We determine the most conservative specifications that this experiment needs, in order to measure the remaining unknown parameters to a specified level of precision. This early physics reach of DUNE can be taken as the aim of the first stage, if the experiment is conducted in a staged approach. For this purpose, we use the latest experimental specifications provided by the collaboration.

In addition, we study the impact of the near detector (ND) in reducing the systematic uncertainties, by explicitly simulating events at both the near detector and the far detector (FD). The role of the near detector and improved systematics used for a superbeamed experiment have been considered in Ref. [72], specifically in the context of the precision measurement of δ_{CP} . We show the effect of systematics for all the three performance indicators—hierarchy, octant, and δ_{CP} , considering the overall signal and background normalization errors at both ND and FD.

We also study the role of the second oscillation maximum in improving the sensitivities, both for DUNE alone and in conjunction with T2K, NO ν A, and ICAL. Optimization of the neutrino and antineutrino run has been studied before in Refs. [51,73]. In this work, the adequate exposure is obtained by assuming equal neutrino and antineutrino runs. Subsequently we also change the proportion of neutrino and antineutrino runs in the adequate exposure and study the optimal combination. This is determined for each of the three unknowns for only DUNE as well as DUNE in conjunction with the LBL experiments T2K and NO ν A and the atmospheric neutrino experiment ICAL@INO.

The plan of the paper is as follows. In Sect. 2, we discuss the configurations of the experiments considered in this work. The next section explores the question posed above – determining the minimal or ‘adequate’ configuration required for DUNE in light of data from T2K, NO ν A, and ICAL, in order to determine the unknown parameters. We then discuss the effect of systematics in Sect. 4 and the significance of the second oscillation maximum for DUNE baseline in Sect. 5. Finally, in Sect. 6, we present an optimization study of the neutrino–antineutrino running at DUNE to get the best possible results.

2 Simulation details

Among the current generation of neutrino oscillation experiments, in this work we consider NO ν A, T2K, and ICAL@INO. NO ν A and T2K are currently operational, while ICAL@INO project has been approved. The precise con-

figuration of DUNE is still being worked on, and in this work we allow its specifications to be variable. For this work, we have simulated the long-baseline experiments using the GLOBES package [74, 75] along with its auxiliary data files [76, 77].

The T2K experiment in Japan shoots a beam of muon neutrinos from J-PARC to the Super-Kamiokande detector in Kamioka, through 295 km of earth. This experiment will run with a total integrated beam strength of around 8×10^{21} pot (protons on target). The specifications used for this detector are as given in Refs. [15, 78–80]. We assume in our study that T2K will run only in the neutrino mode with the above pot. The T2K collaboration has started running in the antineutrino mode. For advantages of neutrino vis-à-vis antineutrino runs we refer to [81, 82]. More discussions of the effect of antineutrino data from T2K will follow in the relevant sections.

The NO ν A experiment at Fermilab takes neutrinos from the NuMI beam, with a beam power of 0.7 MW. The planned run of this experiment is for 6 years, divided into 3 years of neutrino and 3 years of antineutrino mode. The neutrinos are intercepted at the T ASD detector in Ash River, 812 km away and 14 milliradians off the beam axis. The off-axis nature of these experiments helps to impose cuts to reduce the neutral current background. After the measurement of the moderately large value of θ_{13} , the event selection criteria were re-optimized with the intention of exploiting higher statistics [19, 83]. We have used this new configuration for the NO ν A experiment in our work.

ICAL@INO is a magnetized iron detector for observing atmospheric neutrinos [32]. Magnetization allows for a separation of μ^+ and μ^- events, and hence a distinction between neutrinos and antineutrinos. The total exposure taken for this experiment is 500 kiloton year, i.e. 10 years of data collection using a 50 kiloton (kt) detector. We assume an energy resolution of 10 % and angular resolution of 10° for the neutrinos in the detector. These give results comparable to the muon analysis [35, 84] that has been performed by the INO collaboration. The new ‘3-d analysis’, which also includes hadronic energy information [85] is expected to give better results. The statistical procedure followed in calculating the sensitivity of this experiment follows the treatment outlined in Ref. [86].

DUNE is the next generation international neutrino oscillation experiment proposed to be hosted at Fermilab. The beam of neutrinos, with a wide-band profile, will travel 1300 km from Fermilab to a liquid argon detector at SURF, South Dakota. The projected beam power is 1.2 MW with the possibility of upgradation to 2.4 MW. The detailed design of this experiment including beamline, detector, and engineering aspects is expected to rely on the results of R&D work already carried out by earlier proposals including LBNE and LBNO. The higher energy available, along with the long

baseline, means that the neutrinos will experience greater matter effects than NO ν A or T2K. There are two options being considered for the proton beam—80 and 120 GeV. For a given configuration of the beamline and beam power, proton energy varies inversely with the number of protons in the beam per unit time, and hence the neutrino flux. In this work, we have chosen the 120 GeV beam which gives us a lower flux of neutrinos and hence a conservative estimate of our results. The details of the LArTPC detector response have been taken from Ref. [87]. In this work we use the recently updated neutrino flux corresponding to 1.2 MW beam power [88]. However, we give our results in terms of MW-kt-yr. This will enable one to interpret the results in terms of varying detector volume, timescale and beam power. Note that although we use the flux corresponding to 1.2 MW beam power, if the accelerator geometry remains the same, then the change in the value of the beam power will proportionally change the flux. Therefore, the flux for a different value of beam power can be obtained by simply scaling the ‘standard’ flux file by the appropriate factor.

Since DUNE is proposed to be an underground observatory it will also be possible for it to observe atmospheric neutrinos. In this work, we have not considered this possibility. A detailed study on atmospheric neutrinos for the DUNE experiment is presented in Refs. [55, 56].

The sensitivity of DUNE to the mass hierarchy, the octant of θ_{23} , and δ_{CP} comes primarily from the $\nu_\mu \rightarrow \nu_e$ oscillation probability $P_{\mu e}$. An approximate analytical formula for this probability can be derived perturbatively [89–91] in terms of the two small parameters $\alpha = \Delta_{21}/\Delta_{31}$ and $\sin \theta_{13}$.

$$P_{\mu e} = 4 \sin^2 \theta_{13} \sin^2 \theta_{23} \frac{\sin^2 [(1 - \hat{A})\Delta]}{(1 - \hat{A})^2} + \alpha \sin 2\theta_{13} \sin 2\theta_{12} \sin 2\theta_{23} \cos(\Delta + \delta_{CP}) \times \frac{\sin \hat{A}\Delta \sin [(1 - \hat{A})\Delta]}{\hat{A} (1 - \hat{A})} + \mathcal{O}(\alpha^2). \quad (1)$$

Here, $\Delta = \Delta_{31}L/4E$ is the oscillating term, and the effect of neutrinos interacting with matter in the earth is given by the matter term $\hat{A} = 2\sqrt{2}G_F n_e E/\Delta_{31}$, where n_e is the number density of electrons in the earth. Note that this expression is valid in matter of constant density. This approximate formula is useful for understanding the physics of neutrino oscillations. However, in our simulations, we use the full numerical probability calculated by GLOBES.

In the analyses that follow, we have evaluated the χ^2 for determining the mass hierarchy, the octant of θ_{23} , and discovering CP violation¹ using a combination of DUNE and the current/upcoming experiments T2K, NO ν A, and

¹ The commonly used phrase ‘CP-violation discovery’ is taken to mean the distinguishing of a given value of δ_{CP} from the CP-conserving cases 0, 180° . This should not be confused with the statistical usage of the word ‘discovery’ that implies 5σ evidence.

ICAL. For each set of ‘true’ values assumed, we evaluate the χ^2 marginalized over the ‘test’ parameters. In our simulations, we have used the effective atmospheric parameters corrected for three-flavor effects² [92–94]. The true values assumed for the parameters are $\sin^2 \theta_{12} = 0.304$, $|\Delta_{31}| = 2.4 \times 10^{-3} \text{ eV}^2$, $\Delta_{21} = 7.65 \times 10^{-5} \text{ eV}^2$, and $\sin^2 2\theta_{13} = 0.1$. The true value of δ_{CP} is varied throughout the full range $[-180^\circ, 180^\circ]$. For true θ_{23} , we have considered three values— 39° , 45° , and 51° which are within the current 3σ allowed range. The test values of the parameters are varied in the following ranges: $\theta_{23} \in [35^\circ, 55^\circ]$, $\sin^2 2\theta_{13} \in [0.085, 0.115]$, $\delta_{\text{CP}} \in [-180^\circ, 180^\circ]$. The test hierarchy is varied as well. The solar parameters are already measured quite accurately, and their variation does not impact our results significantly. Therefore, we have not marginalized over them. We have imposed a prior of $\sigma(\sin^2 2\theta_{13}) = 0.005$ on the value of $\sin^2 2\theta_{13}$, which is the expected precision from the reactor neutrino experiments [95]. We have included backgrounds arising from NC events, mis-identified ν_μ events, intrinsic beam backgrounds as well as wrong-sign backgrounds. The systematic uncertainties are parameterized in terms of four nuisance parameters—signal normalization error 2.5 % (7.5 %), signal tilt error 2.5 % (2.5 %), background normalization error 10 % (15 %), and background tilt error 2.5 % (2.5 %) for the appearance (disappearance) channel [48].

In Sect. 3, our aim is to economize the configuration of DUNE with the help of the current generation of experiments. We have done that by evaluating the ‘adequate’ exposure for DUNE. The qualifier ‘adequate’, as defined in Ref. [54] in the context of LBNO, means the exposure required from the experiment to determine the hierarchy and octant with $\chi^2 = 25$, and to detect CP violation with $\chi^2 = 9$. To do so, we have varied the exposure of DUNE and determined the combined sensitivity of DUNE along with T2K, NO ν A, and ICAL. The variation of total sensitivity with DUNE exposure tells us what the adequate exposure should be. In this work, we have quantified the exposure for DUNE in units of MW-kt-yr. This is a product of the beam power (in MW), the runtime of the experiment (in years)³ and the detector mass (in kilotons). As a phenomenological study, we will only specify the total exposure in this paper. This may be

² The effective atmospheric mass-squared difference and atmospheric mixing angle are obtained by fitting oscillation data to the effective two-flavor oscillation formula. From a physics point of view, there is no advantage in using these effective parameters and then correcting for three-flavor effects. However, from a computational point of view, we find that the use of these effective parameters gives more precise results while scanning the parameter space, since the hierarchy and octant degeneracies are exact in these parameters.

³ A runtime of n years is to be interpreted as $n/2$ years each in neutrino and antineutrino mode. In this work, we have always considered equal runs in both modes for DUNE unless otherwise mentioned.

interpreted experimentally as different combinations of beam power, runtime and detector mass whose product quantifies the exposure. For example, an exposure of 40 MW-kt-yr could be achieved by using a 10 kt detector for 2 years (in each, the ν and the $\bar{\nu}$ mode), with a 1 MW beam. We use events in the energy range 0.5–10 GeV for DUNE which covers both first and second oscillation maxima. The relative contribution of the second oscillation maximum is discussed in Sect. 5.

3 Adequate exposure for DUNE

3.1 Hierarchy sensitivity

In the left panel of Fig. 1, we have shown the combined sensitivity of DUNE, NO ν A, T2K, and ICAL for determining the mass hierarchy, as the exposure for DUNE is varied. The hierarchy sensitivity typically depends very strongly on the true value of δ_{CP} and θ_{23} . In this work, we are interested in finding out the least exposure needed for DUNE, irrespective of the true values of the parameters in nature. Therefore, we have evaluated the χ^2 for various true values of these parameters as listed in Sect. 2, and taken the most conservative case out of them. Thus, the exposure plotted here is for the most unfavorable values of true δ_{CP} and θ_{23} . Since hierarchy sensitivity of the $P_{\mu e}$ channel increases with θ_{23} , the worst case is usually found at the lowest value considered— $\theta_{23} = 39^\circ$. The most unfavorable of δ_{CP} is around $+(-)90^\circ$ for NH(IH) [18]. Separate curves are shown for both hierarchies, but the results are almost the same in both cases. We find that the adequate exposure for DUNE including T2K, NO ν A, and ICAL data is around 44 MW-kt-yr for both NH and IH. This is shown by the upper curves. The two intermediate curves show the same sensitivity, but without including the ICAL data in the analysis. In this case, the adequate exposure is around 78 MW-kt-yr. Thus, in the absence of ICAL data, DUNE would have to increase its exposure by over 75 % to achieve the same results. For the benchmark values of 1.2 MW power and 10 kt detector, the exposure of 44 MW-kt-yr implies under 2 years of running in each mode whereas the adequate exposure 78 MW-kt-yr corresponds to about 3 years exposure in each mode.

Finally, we show the sensitivity from DUNE alone, in the lower most curves. For the range of exposures considered, DUNE can achieve hierarchy sensitivity up to the $\chi^2 = 16$ level. The first row of Table 1 shows the adequate exposure required for hierarchy sensitivity reaching $\chi^2 = 25$ for only DUNE and also after adding the data from T2K, NO ν A, and ICAL. The numbers in the parentheses correspond to IH. With only DUNE, the exposure required to reach $\chi^2 = 25$ for the hierarchy sensitivity is seen to be much higher.

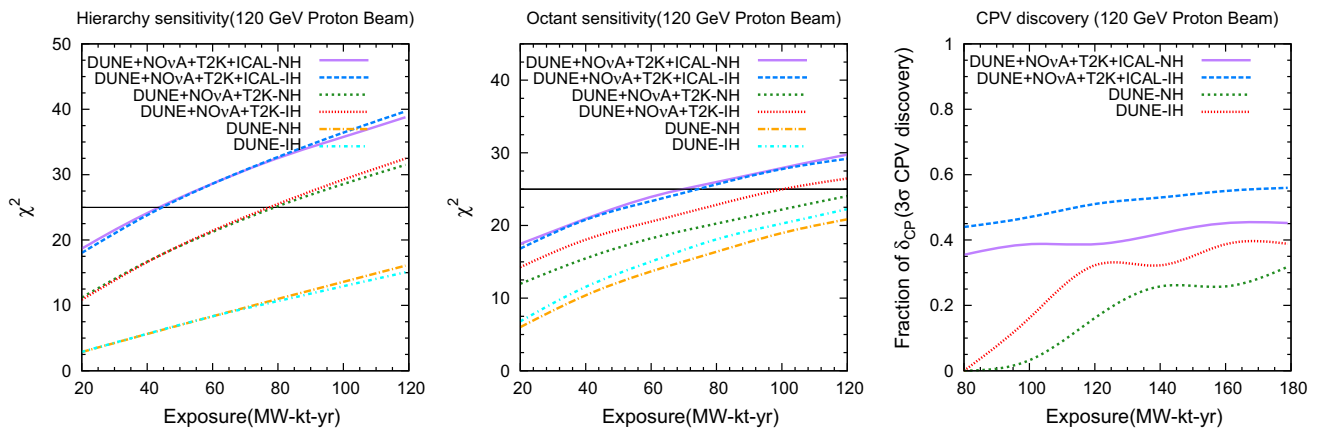


Fig. 1 Hierarchy (octant) sensitivity χ^2 vs. DUNE exposure, for both hierarchies in the *left (middle) panel*. The value of exposure shown here is adequate to exclude the wrong hierarchy (octant) for all values of δ_{CP} . Two additional sets of curves are shown to show the fall in χ^2 without

data from ICAL, and the sensitivity of DUNE alone. The *right panel* shows the fraction of δ_{CP} range for which it is possible to exclude the CP-conserving cases of 0 and 180° , at the $\chi^2 = 9$ level. An additional set of curves is shown to show the CP sensitivity of DUNE alone

Table 1 Adequate exposures for hierarchy, octant and CP in units of MW-kt-yr for NH(IH)

Sensitivity	DUNE + NO ν A + T2K + ICAL	DUNE + NO ν A + T2K	DUNE
Hierarchy ($\chi^2 = 25$)	44 (44)	78 (78)	190 (212)
Octant ($\chi^2 = 25$)	74 (74)	130 (100)	168 (152)
CP (40 % at $\chi^2 = 9$)	130 (72)	130 (72)	228 (180)

3.2 Octant sensitivity

The mass hierarchy as well as the values of δ_{CP} and θ_{23} in nature affect the octant sensitivity of experiments significantly. In our analysis, we have considered various true values of δ_{CP} across its full range, and two representative true values of θ_{23} — 39° and 51° . Having evaluated the minimum χ^2 for each of these cases, we have chosen the lower value. Thus, we have ensured that the adequate exposure shown here holds, irrespective of the true octant of θ_{23} . Note that octant sensitivity reduces as we go more toward $\theta_{23} = 45^\circ$. Thus the above choice of true θ_{23} only corresponds to the more conservative value of θ_{23} out of 39° and 51° .

The middle panel of Fig. 1 shows the combined octant sensitivity of the experiments, as a function of DUNE exposure. Around 70–74 MW-kt-yr for NH(IH) is the required exposure for DUNE, to measure the octant with NO ν A, T2K, and ICAL. This implies a runtime of around 3 years in each mode for the ‘standard’ configuration of DUNE. Without information from ICAL, however, DUNE would have to increase its exposure to around 130(100) MW-kt-yr for NH(IH) to measure the octant with $\chi^2 = 25$. For a 1.2 MW beam and a 10 kt detector this implies about 5(4) years for NH(IH) in each mode. DUNE-only would need a higher exposure of 168 (152) MW-kt-yr for NH(IH) corresponding to about 7(6) years in each mode. Thus including ICAL data reduces the exposure required from DUNE. This is summarized in the second row of Table 1.

3.3 Detecting CP violation

The CP detection ability of an experiment is defined as its ability to distinguish the true value of δ_{CP} in nature from the CP-conserving cases of 0 and 180° . This obviously depends on the true value of δ_{CP} . If δ_{CP} in nature is close to 0 or 180° , this ability will be poor, while if it is close to $\pm 90^\circ$, it will be high. CP detection also depends on θ_{23} , and typically it is a decreasing function of θ_{23} [33]. Here, we have tried to determine the fraction of the entire δ_{CP} range for which our setups can detect CP violation with at least $\chi^2 = 9$. We have always chosen the smallest fraction over various values of θ_{23} (39° , 45° , and 51°), so as to get a conservative estimate.

We find in the right panel of Fig. 1 that for the range of exposures considered, the fraction of δ_{CP} is between 0.35 and 0.55. While the exposure increases by a factor of 2, the increase in the fraction of δ_{CP} is very slow. In Ref. [23], it was shown that the addition of information from ICAL to NO ν A and T2K increases their CP detection ability. This is because ICAL data breaks the hierarchy- δ_{CP} degeneracy that NO ν A and T2K suffer from. However, the DUNE experiment itself is also capable of lifting this degeneracy for most of the values of δ_{CP} [53]. Therefore, the inclusion of ICAL data does not make any difference in this case. This combination of experiments can detect CP violation over 40 % of the δ_{CP} range with an exposure of about 130 MW-kt-yr at DUNE for NH (i.e. a runtime of around 5.5 years in each mode for DUNE with the initial 10 kt detector or around 1.5 years in

Table 2 CPV coverage fraction at 3σ for total 600 MW-Kt-yr exposure

3σ CPV coverage for θ_{23}	DUNE	DUNE + $\text{NO}\nu\text{A}$ + T2K
39°	69 (73)	71 (74)
51°	60 (65)	63 (67)

each mode with the final 40 kt detector). Without including T2K and $\text{NO}\nu\text{A}$ information the exposure required will be 228 MW-kt-yr for 40 % coverage for the discovery of δ_{CP} . As mentioned in the introduction, one of the mandates of DUNE is 3σ CP coverage for 75 % values of δ_{CP} [63]. We find that an exposure of 300 MW-kt-yr in neutrinos and 300 MW-kt-yr in antineutrinos gives 69 % (73 %) CP coverage at 3σ for $\theta_{23} = 39^\circ$ and 60 % (65 %) for 51° in NH(IH). We also find that addition of $\text{NO}\nu\text{A}$ and T2K data does not help much for such high values of exposure. The results are summarized in Table 2.

In the following sections, we fix the exposure in each case to be the adequate exposure as listed in Table 1, for the most conservative parameter values.

4 Role of the near detector in reducing systematics

The measurement of a relatively large value of θ_{13} makes the issue of systematic uncertainties more relevant. The role of the ND in long-baseline neutrino experiments has been well discussed in the literature; see for example Refs. [96–98]. The measurement of events at the ND and FD reduces the uncertainty associated with the flux and cross-section of neutrinos. Thus the role of the near detector is to reduce systematic errors in the oscillation experiment. It has recently been found that the ND for the T2K experiment can bring about a spectacular reduction of systematic errors [99]. The impact of ND and systematic uncertainties in the context of a measurement of the CP violation using appearance channels has been studied in [72, 100] taking the T2HK experiment as an example.

In this study, we have tried to quantify the improvement in results, once the ND is included. The conventional way of doing this is to assume that the existence of the ND leads to a reduction of systematic effects, and therefore input smaller systematic errors by hand in the analysis. Instead of using this approach, we have explicitly simulated the events at the ND using GLOBES. The design for the ND is still being planned. For our simulations, we assume that the ND has a mass of 5 tons and is placed 459 meters from the source. The flux at the ND site has been provided by the DUNE collaboration [88]. The detector characteristics for the ND are as follows [101]. The muon (electron) detection efficiency is taken to be 95 % (50 %). The NC background can be

rejected with an efficiency of 20 %. The energy resolution for electrons is $6\%/\sqrt{E(\text{GeV})}$, while that for muons is 37 MeV across the entire energy range of interest. Therefore, for the neutrinos, we use a (somewhat conservative) energy resolution of $20\%/\sqrt{E(\text{GeV})}$. The systematic errors that the ND setup suffers from are assumed to be the same as those from the FD.

In order to have equal runtime for both FD and ND, we fix the FD volume as 10 kt and consider both detectors to receive neutrinos from 1.2 MW beam. This fixes the runtime of FD, which is then also used in the simulation for ND. The run times used in this section are chosen corresponding to the adequate exposures from the previous section as given in the first column of Table 1: 3.6 year for hierarchy sensitivity, 6.2 year for octant sensitivity and 10.8 year for CPV discovery sensitivity.

In order to simulate the ND+FD setup for DUNE, we use GLOBES to generate events at both detectors, treating them as separate experiments. We then use these two data sets to perform a correlated systematics analysis using the method of pulls [102]. This gives us the combined sensitivity of DUNE using both ND and FD. (We have explained our methodology in Appendix A.) Thereafter, the procedure of combining results with other experiments and marginalizing over oscillation parameters continues in the usual manner. The results are shown in Fig. 2. The effect of reduced systematic errors is felt most significantly in regions where the results are best. This is because for those values of δ_{CP} , the experiment typically has high enough statistics for systematic errors to play an important role.

Next, we have tried to quantify the reduction in systematic errors seen by the experiment, when the ND is included. To be more specific, if the systematic errors seen by each detector setup are denoted by π , then we wonder what is the effective set of errors π_{eff} for the FD setup, once the ND is also included. In other words, for given systematic errors π , we have found the effective errors π_{eff} that satisfy the relation

$$\chi^2(\text{FD}(\pi_{\text{eff}})) \equiv \chi^2(\text{FD}(\pi) \oplus \text{ND}(\pi)), \quad (2)$$

where the right-hand side denotes the correlated combination as described in Appendix A. The π_{eff} thus computed can be used in future simulations as the reduced set of systematic errors because of the presence of the ND. We have chosen typical values of systematic errors for the detector: the ν_e appearance signal normalization error of 2.5 %, the ν_μ disappearance signal normalization error of 7.5 %, the ν_e appearance background normalization error of 10 % and the ν_μ disappearance background normalization error of 15 %. The tilt error is taken as 2.5 % in both appearance and disappearance channels. The first four numbers constitute π , as labeled in the figure. We find that the tilt errors have a very

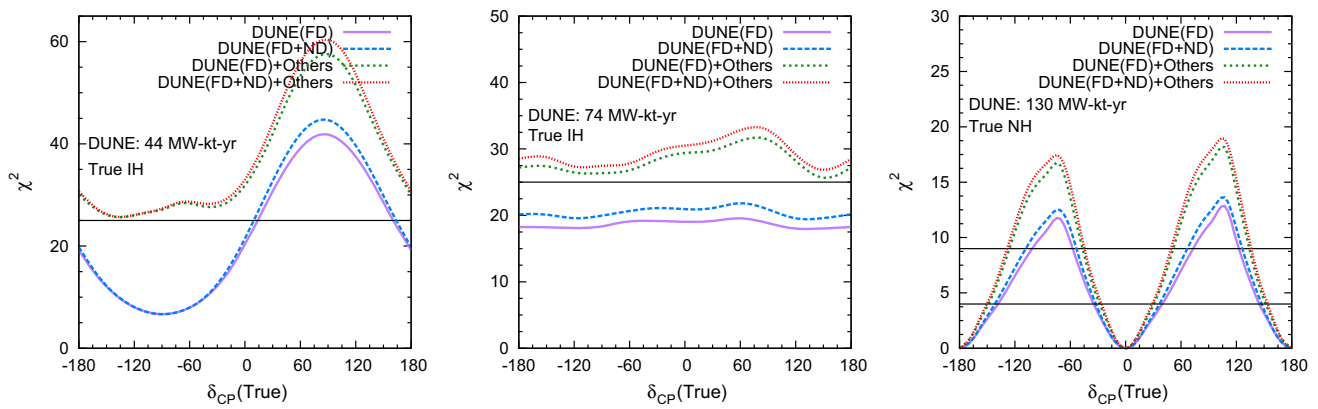


Fig. 2 Hierarchy/octant/CP violation discovery sensitivity χ^2 vs. true δ_{CP} in the *left/middle/right panel*. The various *curves* show the effect of including a near detector on the sensitivity of DUNE alone and DUNE combined with the other experiments

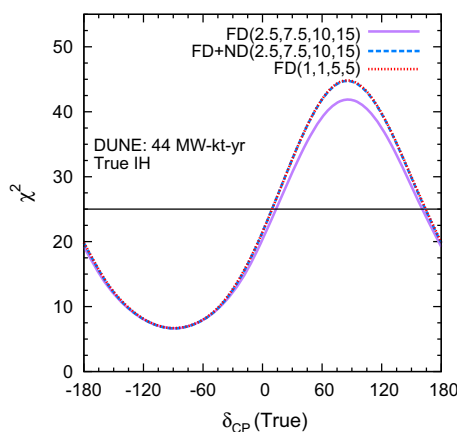


Fig. 3 Reduction in systematics due to inclusion of the near detector. The *numbers in brackets* denote the ν_e appearance signal normalization error, the ν_μ disappearance signal normalization error, the ν_e appearance background normalization error, and the ν_μ disappearance background normalization error

small effect in this particular analysis, and we fix them to the value specified above. The result of the computation is shown in Fig. 3, for the case of hierarchy determination. The sensitivity of FD + ND obtained using these numbers, are matched by an FD setup with effective errors as follows: a ν_e appearance signal normalization error of 1 %, a ν_μ disappearance signal normalization error of 1 %, a ν_e appearance background normalization error of 5 %, and a ν_μ disappearance background normalization error of 5 %. Similar results are obtained in the case of octant and CP sensitivity also. Thus, inclusion of the ND brings the systematic errors down to 13–50 % of their original value. These results are summarized in Table 3. Note that the numbers presented in Table 3 are indicative assuming the systematic uncertainties are energy independent. However, the improvement in the systematic uncertainties in the actual analysis incorporate this energy dependence due to a full bin-by-bin analysis of the ND data.

Table 3 Reduction in systematic errors with the addition of a near detector

Systematic error	Only FD (%)	FD + ND (%)
ν_e app signal norm error	2.5	1
ν_μ disapp signal norm error	7.5	1
ν_e app background norm error	10	5
ν_μ disapp background norm error	15	5

5 Significance of the second oscillation maximum

For a baseline of 1300 km, the oscillation probability $P_{\mu e}$ has its first oscillation maximum around 2–2.5 GeV. This is easy to explain from the formula

$$\frac{\Delta_{31}^{(m)} L}{4E} = \frac{\pi}{2},$$

where $\Delta_{31}^{(m)}$ is the matter-modified atmospheric mass-squared difference. In the limit $\Delta_{21} \rightarrow 0$, it is given by

$$\Delta_{31}^{(m)} = \Delta_{31} \sqrt{(1 - \hat{A})^2 + \sin^2 2\theta_{13}}.$$

The second oscillation maximum, for which the oscillating term takes the value $3\pi/2$, occurs at an energy of around 0.6–1.0. Studies have discussed the advantages of using the second oscillation maximum to get information on the oscillation parameters [73, 103]. In fact, one of the main aims of the proposed ESSnuSB project [104, 105] is to study neutrino oscillations at the second oscillation maximum.

The neutrino flux that DUNE will use has a wide-band profile, which can extract physics from both, the first and second maxima. Figure 4 shows $P_{\mu e}$ for the DUNE baseline, superimposed on the ν_μ flux. This is in contrast with NO ν A, which uses a narrow-band off-axis beam concentrating on its first oscillation maximum, in order to reduce the π^0 background at higher energies.

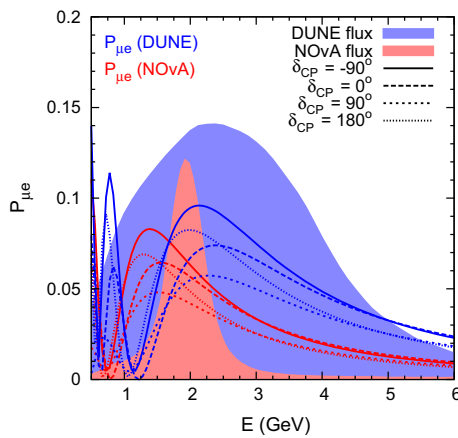


Fig. 4 Neutrino oscillation probability $P_{\mu e}$ for various representative values of δ_{CP} and normal hierarchy, for the NOvA and DUNE baselines. Also shown as shaded profiles in the background are the ν_{μ} flux for both these experiments (on independent, arbitrary scales)

In order to understand the impact of the second oscillation maximum, we have considered two different energy ranges. Above 1.1 GeV, only the first oscillation cycle is relevant. However, if we also include the energy range from 0.5 to 1.1 GeV, we also get information from the second oscillation maximum. Figure 5 compares the sensitivity to the hierarchy, octant and CP violation only from the first oscillation cycle, and from both oscillation cycles assuming the adequate exposures obtained in the previous section. We see that inclusion of data from the second oscillation maximum only increases the χ^2 by a small amount. This increase is visible only for hierarchy sensitivity. The effect is seen to be more pronounced in the region $\delta_{CP} \sim -90^\circ$. This is because the probability for $\{IH, \delta_{CP} = -90^\circ\}$ is closer to that for $\{NH, \delta_{CP} = +90^\circ\}$ at the first oscillation maximum, as reflected in the first panel of Fig. 6. But at the second oscillation maximum the separation between the probabilities for these two sets is higher. Therefore adding the second oscillation maximum aids the hierarchy sensitivity.

In the right panel of Fig. 6 we show how the exposure for hierarchy sensitivity depends on the inclusion of the second oscillation maximum for only DUNE and DUNE + T2K + NOvA + ICAL. It is clear from the figure that the second maximum plays a more significant role for higher exposure. For the combined case, 5σ sensitivity is reached at a relatively lower exposure and hence the second maximum does not play a major role. This is also seen in Fig. 5. However, only for DUNE, since 5σ sensitivity is reached for a relatively higher exposure, the inclusion of the second oscillation maximum is seen to play an important role. This feature is reflected in Table 4.

6 Optimizing the neutrino–antineutrino runs

One of the main questions while planning any beam-based neutrino experiment is the ratio of neutrino to antineutrino run. Since the dependence of the oscillation parameters on the neutrino and antineutrino probabilities are different, an antineutrino run can provide a different set of data which may be useful in the determination of the parameters. However, the interaction cross-section for antineutrinos in the detectors is smaller by a factor of 2.5–3 than the neutrino cross-sections. Therefore, an antineutrino run typically has lower statistics. Thus, the choice of neutrino–antineutrino ratio is often a compromise between new information and statistics.

It is now well known that neutrino and antineutrino oscillation probabilities suffer from the same form of hierarchy- δ_{CP} degeneracy [18]. However, the octant- δ_{CP} degeneracy has the opposite form for neutrinos and antineutrinos [20, 24]. Thus, inclusion of an antineutrino run helps in lifting this degeneracy for most of the values of δ_{CP} [53]. For measurement of δ_{CP} , it has been shown for T2K that the antineutrino run is required only for those true hierarchy-octant- δ_{CP} combination for which octant degeneracy is present [81]. Once this

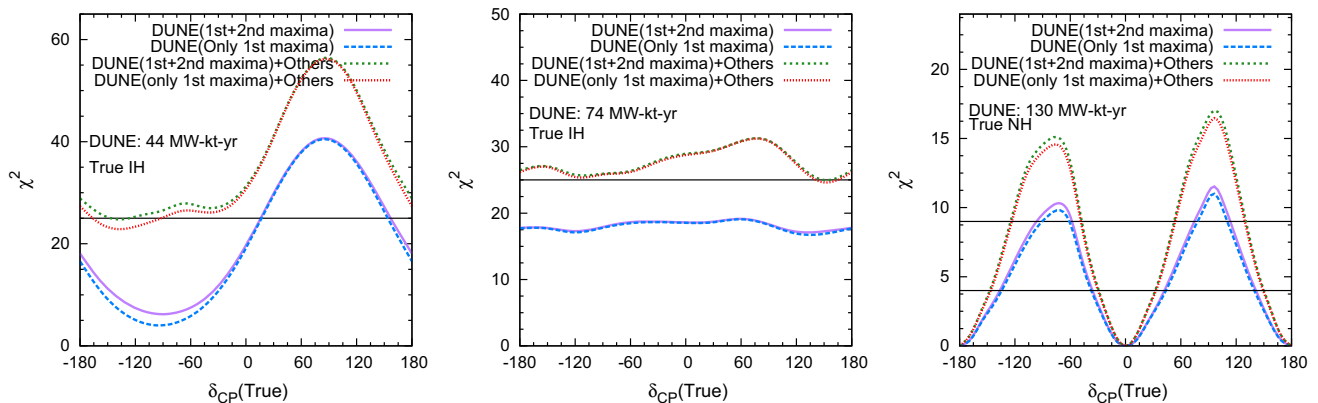


Fig. 5 Hierarchy/octant/CP violation discovery sensitivity χ^2 vs. true δ_{CP} in the left/middle/right panel. The various curves show the effect of data from the second oscillation maximum on the sensitivity of DUNE alone and DUNE combined with the other experiments

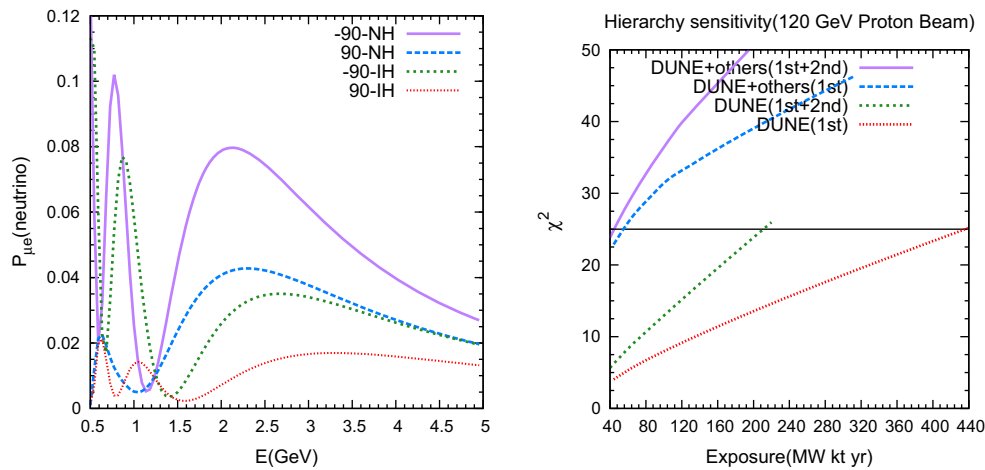


Fig. 6 *Left panel* The probability vs. energy showing the hierarchy- δ_{CP} degeneracy affecting the hierarchy sensitivity at the two oscillation maxima. *Right panel* Hierarchy exclusion χ^2 vs. exposure, with and without the second oscillation maximum

Table 4 Effect of the second oscillation maximum on the sensitivity of DUNE

Sensitivity	DUNE+NO ν A+T2K+ICAL (MW-kt-yr)		Only DUNE (MW-kt-yr)	
	1st + 2nd osc. cycles	Only 1st osc. cycle	1st + 2nd osc. cycles	Only 1st osc. cycle
Hierarchy ($\chi^2 = 25$)	44	56	212	436
Octant ($\chi^2 = 25$)	74	78	168	190
CP (40 % coverage at $\chi^2 = 9$)	130	140	228	256

The numbers indicate the adequate exposure (in MW-kt-yr) required by DUNE for determining the oscillation parameters, with and without the contribution from the second oscillation maximum. For each of the three unknowns, the true parameters (including hierarchy) are taken to be ones for which we get the most conservative sensitivity

degeneracy is lifted by including some amount of antineutrino data, further antineutrino run does not help much in CP discovery; in fact it is then better to run with neutrinos to gain in statistics [81]. But this conclusion may change for a different baseline and matter effect. From Fig. 4 we see that for NO ν A the oscillation peak does not coincide with the flux peak. Around the energy where the flux peaks, the probability spectra with $\delta_{CP} = \pm 0, 180^\circ$ are not equidistant from the $\delta_{CP} = \pm 90^\circ$ spectra. For antineutrino mode the curves for $\pm 90^\circ$ switch position. Hence for neutrinos $\delta_{CP} = 0^\circ$ is closer to $\delta_{CP} = -90^\circ$ and $\delta_{CP} = 180^\circ$ is closer to $\delta_{CP} = 90^\circ$, while the opposite is true for antineutrinos. This gives a synergy and hence running in both neutrino and antineutrino modes can be helpful. For T2K the energy where the flux peak occurs coincides with the oscillation peak. At this point the curves for $\delta_{CP} = 0, 180^\circ$ are equidistant from $\delta_{CP} = \pm 90^\circ$ and hence this synergy is not present. Thus, the role of antineutrino run is only to lift the octant degeneracy. The recent hint of δ_{CP} from T2K [14] already gives us some evidence of the octant (see Table XXVIII in Ref. [106], or Ref. [81]). Moreover, NO ν A and DUNE will collect far more data with antineutrinos than T2K. Thus, the inclusion of antineutrino run at T2K does not make much difference to our results. In the following we have varied the proportion of

neutrino and antineutrino runs at DUNE to ascertain what is the optimal combination. The adequate exposure is split into various combinations of neutrinos and antineutrinos – $1/6 \nu + 5/6 \bar{\nu}$, $2/6 \nu + 4/6 \bar{\nu}$, ... $6/6 \nu + 0/6 \bar{\nu}$. The intermediate configuration $3/6 \nu + 3/6 \bar{\nu}$ corresponds to the equal-run configuration used in the other sections. For convenience of notation, these configurations are referred to simply as 1 + 5, etc., i.e. without appending the ‘/6’. The results are shown in Fig. 7.

The top row of Fig. 7 shows the hierarchy sensitivity of DUNE for various combinations of neutrino and antineutrino run. Normal hierarchy and $\theta_{23} = 39^\circ$ have been assumed as the true parameters. For DUNE, we have chosen a total exposure of 44 MW-kt-yr which was found to be the adequate exposure in Sect. 3 assuming equal neutrino and antineutrino runs. In the left panel, we see the results for DUNE alone. The figure shows that in the favorable region of $\delta_{CP} \in [-180^\circ, 0]$ the best sensitivity comes from the combination 3 + 3 or 4 + 2. Although the statistics is more for neutrinos, the antineutrino run is required to remove the wrong-octant regions. For NH, $\delta_{CP} \in [0, 180^\circ]$ is the unfavorable region for hierarchy determination [18], as is evident from the figure. In this region, we see that the results are worst for pure neutrino run. The best sensitivity comes for the case 5 + 1. This amount

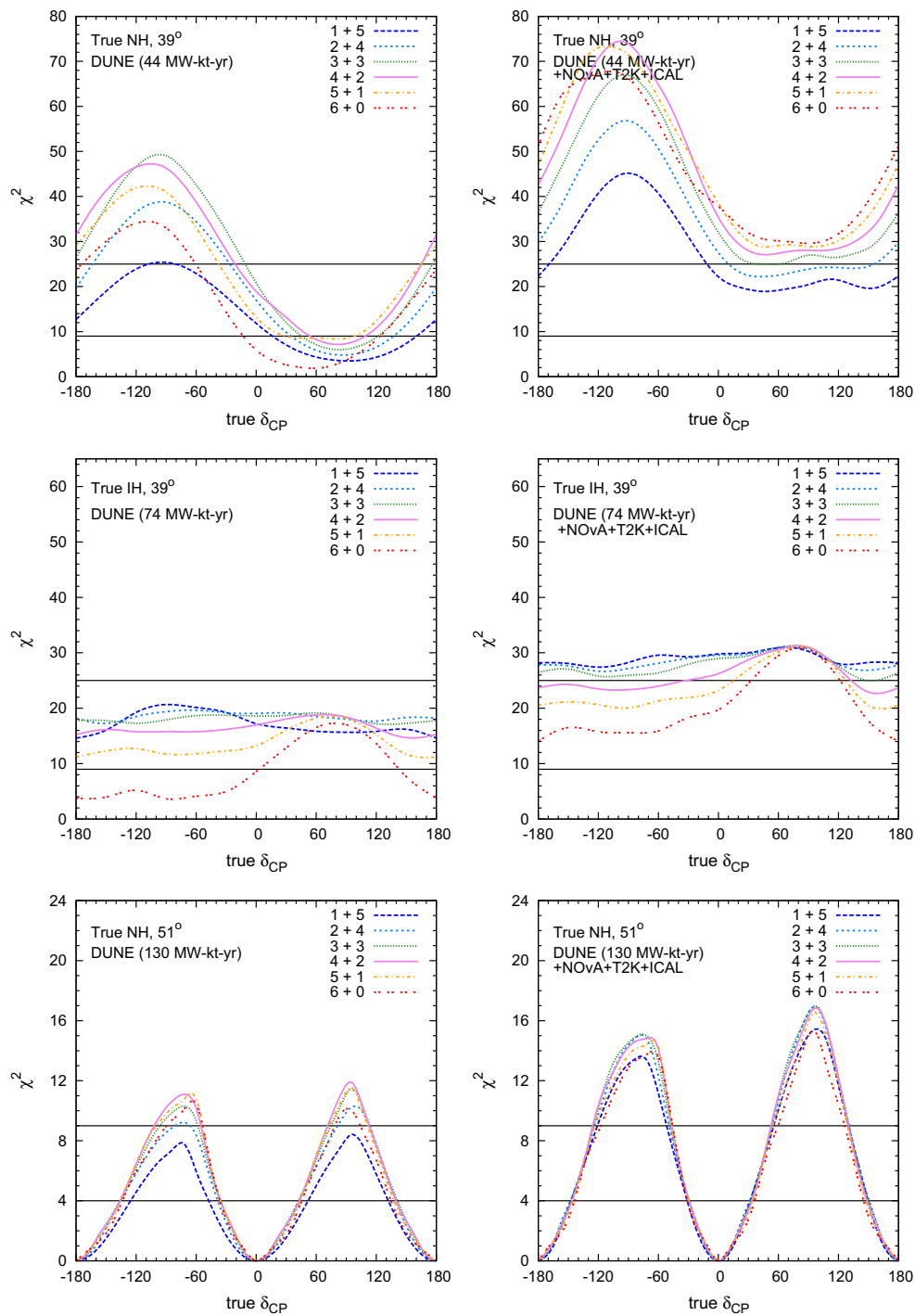


Fig. 7 Sensitivity for DUNE for various combinations of neutrino and antineutrino run by itself (*left panel*) and in conjunction with T2K, NOvA, and ICAL (*right panel*). The *top/middle/bottom* row shows the sensitivity to hierarchy/octet/CP violation detection. The total expo-

sure has been divided into 6 equal parts and distributed between neutrinos and antineutrinos. For example, for hierarchy sensitivity, 6 + 0 corresponds to 44 MW-kt-yr in only neutrino; 3 + 3 correspond to 22 MW-kt-yr in each neutrino and antineutrino mode

of antineutrino run is required to remove the octant degeneracy. The higher proportion of neutrino run ensures better statistics. In the right panel, along with DUNE we have also combined data from NOvA, T2K, and ICAL. With the inclu-

sion of these data the hierarchy sensitivity increases further and even in the unfavorable region $\chi^2 = 25$ sensitivity is possible with only neutrino run from DUNE. This is because NOvA, which will run in antineutrino mode for 3 years and

the antineutrino component in the atmospheric neutrino flux at ICAL, will provide the necessary amount of information to lift the parameter degeneracies that reduce hierarchy sensitivity. Therefore, the best option for DUNE is to run only in neutrino mode, which will have the added advantage of increased statistics. In the favorable region also the sensitivity is now better for $6 + 0$ and $5 + 1$ i.e. less amount of antineutrinos from DUNE is required because of the antineutrino information coming from $\text{NO}\nu\text{A}$. Note that overall, the amount of antineutrino run depends on the value of δ_{CP} . However, combining information from all the experiments $4 + 2$ seems to be the best option over the largest fraction of δ_{CP} values.

In the middle row of Fig. 7, we have shown the octant sensitivity of DUNE alone (left panel) and in combination with the current experiments (right panel). For DUNE we have used an exposure of 74 MW-kt-yr. We have fixed the true hierarchy to be inverted, and $\theta_{23} = 39^\circ$ i.e. in the lower octant. For this case the probability for neutrinos is maximum for $\delta_{\text{CP}} \sim -90^\circ$ and overlaps with the higher octant probabilities. Thus the octant sensitivity in neutrino channel is very poor. This the worst results for these values of δ_{CP} come from only neutrino runs. For antineutrino channel because of the flip in δ_{CP} the probability for $\delta_{\text{CP}} = -90^\circ$ is well separated from those for HO. Therefore the octant sensitivity comes mainly from antineutrino channel [20]. Thus, addition of antineutrino runs help in enhancing octant sensitivity. Therefore at -90° the best sensitivity is from $1 + 5$ i.e. 1/6th neutrino + 5/6th antineutrino combination. On the other hand the neutrino probability is minimum for $\delta_{\text{CP}} = +90^\circ$ and LO and therefore there is octant sensitivity in the neutrino channel. However, since we are considering IH the antineutrino probabilities are enhanced due to matter effect and for a broadband beam some sensitivity comes from the antineutrino channel also. Therefore there is a slight increase in the octant sensitivity by adding antineutrino data as can be seen. Overall, the best compromise is seen to be reached for $2 + 4$ i.e. 1/3rd neutrino and 2/3rd antineutrino combination, which gives the best results over the widest range of δ_{CP} values. Addition of $\text{NO}\nu\text{A}$, T2K, and ICAL data increases the octant sensitivity. The octant sensitivity is best for combinations having more antineutrinos. For $\delta_{\text{CP}} \sim +90^\circ$ all combinations give almost the same sensitivity. We have not presented the results for NH in this case. For this case after adding T2K+ $\text{NO}\nu\text{A}$ +ICAL to DUNE requires at least $4 + 2$ to reach $\chi^2 = 25$ for $\delta_{\text{CP}} \in [-180^\circ, 0]$ while for $\delta_{\text{CP}} \in [0, 180^\circ]$ the octant sensitivity almost crosses $\chi^2 = 25$ for all combinations of neutrino and antineutrino run. Therefore, the exact combination chosen does not make much difference to the final result.

The left and right panels of the bottom row in Fig. 7 show the ability of DUNE (by itself, and in conjunction with the current generation of experiments, respectively) to detect CP

violation. Here the true hierarchy is NH and true θ_{23} is 51° . Although this true combination does not suffer from any octant degeneracy, we see in the left panel that $6 + 0$ is not the best combination. This is due to the synergy between neutrino–antineutrino runs for larger baselines as discussed earlier. In both cases, we find that the best option is to run DUNE with antineutrinos for around a third of the total exposure. On adding information from T2K and $\text{NO}\nu\text{A}$, we find great improvement in the CP sensitivity. From the right panel, we see that the range of δ_{CP} for which $\chi^2 = 9$ detection of CP is possible is almost the same for most combinations of neutrino and antineutrino run. Therefore, as in the case of octant determination, the exact choice of combination is not very important.

7 Summary

The DUNE experiment at Fermilab has a promising physics potential. Its baseline is long enough to see matter effects which will help it to break the δ_{CP} -related degeneracies and determine the neutrino mass hierarchy and the octant of θ_{23} . This experiment is also known to be good for detecting CP violation in the neutrino sector. The current and upcoming experiments T2K, $\text{NO}\nu\text{A}$, and ICAL@INO will also provide some indications for the values of the unknown parameters. In this work, we have explored the physics reach of DUNE, given the data that these other experiments will collect. We have evaluated the adequate exposure for DUNE (in units of MW-kt-yr), i.e. the minimum exposure for DUNE to determine the unknown parameters in combination with the other experiments, for all values of the oscillation parameters. The threshold for the determination is taken to be $\chi^2 = 25$ for the mass hierarchy and octant, and $\chi^2 = 9$ for detecting CP violation. The results are summarized in Table 1. We find that adding information from $\text{NO}\nu\text{A}$ and T2K helps in reducing the exposure required by only DUNE for determination of all the three unknowns—hierarchy, octant and δ_{CP} . Adding ICAL data to this combination further help in achieving the same level of sensitivity with a reduction in exposure of DUNE (apart from δ_{CP}). Thus the synergy between various experiments can be helpful in economizing the DUNE configuration. We have also probed the role of the ND in improving the results by reducing systematic errors. We have simulated events at the near and far detectors and performed a correlated systematics analysis of both sets of events. We find an improvement in the physics reach of DUNE when the ND is included. We have also evaluated the drop in systematics because of the near detector. Our results are shown in Table 3.

Further we have checked the role of information from the lowest energy bins which are affected by the second oscillation maximum of the probability. We find that inclusion of these bins enhances the hierarchy sensitivity since the

hierarchy- δ_{CP} degeneracy has a complementary behavior at the two oscillation maxima. Thus the increase in sensitivity is most significant in regions of parameter space where the degeneracies reduce the sensitivity. We find that the effect is more prominent when a greater exposure is required. For the combined analysis to reach $\chi^2 = 25$ one needs, respectively, 44 (56) MW-kt-yr including (excluding) the second oscillation maximum. However, for only DUNE the same sensitivity requires 436 MW-kt-yr but including the second oscillation maximum the exposure is reduced to 212 MW-kt-yr to reach $\chi^2 = 25$.

Finally, we have done an optimization study of the neutrino-antineutrino run for DUNE. The amount of antineutrino run required depends on the true value of δ_{CP} . It helps in achieving two objectives—(i) reduction in octant degeneracy and (ii) synergy between neutrino and antineutrino data for octant and CP sensitivity.

For a hierarchy determination using a total exposure of 44 MW-kt-yr the optimal combination for only DUNE is (3+3), which corresponds to 22 MW-kt-yr in neutrino and antineutrino mode each, for δ_{CP} in the lower half-plane $[-180^\circ, 0]$ and true NH-LO. For δ_{CP} in the upper half-plane $([0, 180^\circ])$ the optimal ratio is 5/6th of the total exposure in neutrinos and +1/6th of the total exposure in antineutrinos. Adding information from T2K, NO ν A, and ICAL the best combination for DUNE is 2/3rd neutrino + 1/3rd antineutrino for δ_{CP} in the lower half-plane. In the upper half-plane, pure neutrino run gives the best sensitivity. In the latter case, the antineutrino component coming from NO ν A and ICAL helps in reducing the required antineutrino run from DUNE. For octant sensitivity the best result from the combined experiments comes from the proportion (1/6th + 5/6th) except for $\delta_{CP} = +90^\circ$ where all combinations give almost the same sensitivity. For δ_{CP} all combinations give similar results when all data are added together, with equal neutrino and antineutrino or 2/3rd neutrino + 1/3rd antineutrino combination faring slightly better.

To conclude, the DUNE experiment can measure mass hierarchy, octant and δ_{CP} with considerable precision. Inclusion of the data from the experiments like T2K, NO ν A, and ICAL can help DUNE to attain the same level of precision with a reduced exposure. Thus the synergistic aspects between different experiments can help in the planning of a more economized configuration for DUNE.

Acknowledgments We would like to thank Daniel Cherdack, Raj Gandhi, Newton Nath and Robert Wilson for useful discussions.

Open Access This article is distributed under the terms of the Creative Commons Attribution 4.0 International License (<http://creativecommons.org/licenses/by/4.0/>), which permits unrestricted use, distribution, and reproduction in any medium, provided you give appropriate credit to the original author(s) and the source, provide a link to the Creative Commons license, and indicate if changes were made. Funded by SCOAP³.

Appendix A: Computing the effect of the near detector on systematics

In this appendix, we discuss briefly the simple procedure that we have used to combine results from the ND and FD, with correlated systematics. This procedure is based on the method of pulls [102]. The (1σ) systematic errors are given by a set of numbers $\boldsymbol{\pi}$. These errors can be normalization errors (which affect the scaling of events) or tilt errors (which affect the energy dependence of the events). The ‘experimental’ data $N_i^{\text{det(ex)}}$ are simulated using the ‘true’ oscillation parameters \mathbf{p}_{ex} , while the ‘theoretical’ events $N_i^{\text{det(th)}}$ are generated using the ‘test’ oscillation parameters \mathbf{p}_{th} . The subscript i here runs over all the energy bins. The superscript det can take values ND or FD. The theoretical events get modified due to systematic errors as

$$M_i^{\text{det(th)}}(\mathbf{p}_{\text{th}}) = N_i^{\text{det(th)}}(\mathbf{p}_{\text{th}}) \left[1 + \sum_k \xi_k \pi^k + \sum_l \xi_l \pi^l \frac{E_i - E_{\text{av}}}{E_{\text{max}} - E_{\text{min}}} \right],$$

where the index $k(l)$ runs over the relevant normalization (tilt) systematic errors for a given experimental observable. All the pull variables $\{\xi_j\}$ take values in the range $(-3, 3)$, so that the errors can vary from -3σ to $+3\sigma$. Here, E_i is the mean energy of the i th energy bin, E_{min} and E_{max} are the limits of the full energy range, and E_{av} is their average.

The Poissonian χ^2 is calculated for each detector as

$$\chi^2_{\text{det}}(\mathbf{p}_{\text{ex}}, \mathbf{p}_{\text{th}}; \{\xi_j\}) = \sum_i 2 \left[M_i^{\text{det(th)}}(\mathbf{p}_{\text{th}}) - N_i^{\text{det(ex)}}(\mathbf{p}_{\text{ex}}) + N_i^{\text{det(ex)}}(\mathbf{p}_{\text{ex}}) \ln \left(\frac{N_i^{\text{det(ex)}}(\mathbf{p}_{\text{ex}})}{M_i^{\text{det(th)}}(\mathbf{p}_{\text{th}})} \right) \right].$$

The results from the two detector setups are then combined, along with a penalty for each source of systematic error. The final χ^2 is calculated by minimizing over all combinations of ξ_j ,

$$\begin{aligned} \chi^2(\mathbf{p}_{\text{ex}}, \mathbf{p}_{\text{th}}) &= \min_{\{\xi_j\}} \left[\chi^2_{\text{FD}}(\mathbf{p}_{\text{ex}}, \mathbf{p}_{\text{th}}; \{\xi_j\}) \right. \\ &\quad \left. + \chi^2_{\text{ND}}(\mathbf{p}_{\text{ex}}, \mathbf{p}_{\text{th}}; \{\xi_j\}) + \sum_j \xi_j^2 \right] \\ &\equiv \chi^2(\text{FD} \oplus \text{ND}). \end{aligned}$$

Usually, for two experiments with uncorrelated systematics, the adding of penalties and minimizing over the pull variables is done independently, and the resulting χ^2 values are added. In contrast, here we add the same pulls to both detector setups, and then minimize over the pull variables.

This takes care of correlations between the systematic effects of the two setups.

References

- Super-Kamiokande, S. Fukuda et al., Phys. Lett. B **539**, 179 (2002). [arXiv:hep-ex/0205075](#)
- SNO, Q.R. Ahmad et al., Phys. Rev. Lett. **89**, 011301 (2002). [arXiv:nucl-ex/0204008](#)
- SNO, B. Aharmim et al., Phys. Rev. C **72**, 055502 (2005). [arXiv:nucl-ex/0502021](#)
- KamLAND, K. Eguchi et al., Phys. Rev. Lett. **90**, 021802 (2003). [arXiv:hep-ex/0212021](#)
- Super-Kamiokande Collaboration, R. Wendell et al., Phys. Rev. D **81**, 092004 (2010). [arXiv:1002.3471](#)
- MINOS Collaboration, P. Adamson et al., Phys. Rev. Lett. **112**, 191801 (2014). [arXiv:1403.0867](#)
- T2K Collaboration, K. Abe et al., Phys. Rev. Lett. **111**, 211803 (2013). [arXiv:1308.0465](#)
- Double Chooz Collaboration, Y. Abe et al., JHEP **1410**, 86 (2014). [arXiv:1406.7763](#)
- Daya Bay Collaboration, F. An et al., Phys. Rev. Lett. **112** 061801 (2014). [arXiv:1310.6732](#)
- RENO collaboration, J. Ahn et al., Phys. Rev. Lett. **108**, 191802 (2012). [arXiv:1204.0626](#)
- F. Capozzi et al., Phys. Rev. D **89**, 093018 (2014). [arXiv:1312.2878](#)
- D. Forero, M. Tortola, J. Valle, Phys. Rev. D **90**, 093006 (2014). [arXiv:1405.7540](#)
- M. Gonzalez-Garcia, M. Maltoni, T. Schwetz, JHEP **1411**, 052 (2014). [arXiv:1409.5439](#)
- T2K, K. Abe et al., Phys. Rev. Lett. **112**, 061802 (2014). [arXiv:1311.4750](#)
- T2K, Y. Itow et al. (2001). [arXiv:hep-ex/0106019](#)
- NOvA Collaboration, D. Ayres et al. (2004). [arXiv:hep-ex/0503053](#)
- P. Huber et al., JHEP **11**, 044 (2009). [arXiv:0907.1896](#)
- S. Prakash, S.K. Raut, S.U. Sankar, Phys. Rev. D **86**, 033012 (2012). [arXiv:1201.6485](#)
- S.K. Agarwalla et al., JHEP **1212**, 075 (2012). [arXiv:1208.3644](#)
- S.K. Agarwalla, S. Prakash, S.U. Sankar, JHEP **1307**, 131 (2013). [arXiv:1301.2574](#)
- S. Prakash, U. Rahaman, S.U. Sankar, JHEP **07**, 070 (2014). [arXiv:1306.4125](#)
- A. Chatterjee et al., JHEP **1306**, 010 (2013). [arXiv:1302.1370](#)
- M. Ghosh et al., Phys. Rev. D **89**, 011301 (2014). [arXiv:1306.2500](#)
- P. Machado et al., JHEP **1405**, 109 (2014). [arXiv:1307.3248](#)
- P. Coloma, H. Minakata, S.J. Parke, Phys. Rev. D **90**, 093003 (2014). [arXiv:1406.2551](#)
- M. Ghosh et al., Phys. Rev. D **93**, 013013 (2016). [arXiv:1504.06283](#)
- J. Elevant, T. Schwetz, JHEP **09**, 016 (2015). [arXiv:1506.07685](#)
- A.M. Ankowski et al., Phys. Rev. D **92**, 091301 (2015). [arXiv:1507.08561](#)
- P. Huber, M. Lindner, W. Winter, Nucl. Phys. B **654**, 3 (2003). [arXiv:hep-ph/0211300](#)
- H. Minakata, H. Sugiyama, Phys. Lett. B **580**, 216 (2004). [arXiv:hep-ph/0309323](#)
- O. Mena, S.J. Parke, Phys. Rev. D **70**, 093011 (2004). [arXiv:hep-ph/0408070](#)
- ICAL, S. Ahmed et al. (2015). [arXiv:1505.07380](#)
- M. Ghosh et al., Nucl. Phys. B **884**, 274 (2014). [arXiv:1401.7243](#)
- M. Blennow, T. Schwetz, JHEP **1208**, 058 (2012). [arXiv:1203.3388](#)
- A. Ghosh, T. Thakore, S. Choubey, JHEP **1304**, 009 (2013). [arXiv:1212.1305](#)
- V. Barger, D. Marfatia, K. Whisnant, Phys. Rev. D **65**, 073023 (2002). [arXiv:hep-ph/0112119](#)
- V. Barger, D. Marfatia, K. Whisnant, Phys. Rev. D **66**, 053007 (2002). [arXiv:hep-ph/0206038](#)
- H. Minakata, H. Nunokawa, JHEP **0110**, 001 (2001). [arXiv:hep-ph/0108085](#)
- J. Burguet-Castell et al., Nucl. Phys. B **646**, 301 (2002). [arXiv:hep-ph/0207080](#)
- H. Minakata, H. Nunokawa, S.J. Parke, Phys. Rev. D **66**, 093012 (2002). [arXiv:hep-ph/0208163](#)
- G.L. Fogli, E. Lisi, Phys. Rev. D **54**, 3667 (1996). [arXiv:hep-ph/9604415](#)
- M. Ishitsuka et al., Phys. Rev. D **72**, 033003 (2005). [arXiv:hep-ph/0504026](#)
- T. Kajita et al., Phys. Rev. D **75**, 013006 (2007). [arXiv:hep-ph/0609286](#)
- K. Hagiwara, N. Okamura, K.I. Senda, Phys. Lett. B **637**, 266 (2006). [arXiv:hep-ph/0504061](#)
- O. Mena Requejo, S. Palomares-Ruiz, S. Pascoli, Phys. Rev. D **72**, 053002 (2005). [arXiv:hep-ph/0504015](#)
- O. Mena, S. Palomares-Ruiz, S. Pascoli, Phys. Rev. D **73**, 073007 (2006). [arXiv:hep-ph/0510182](#)
- V. Barger, D. Marfatia, K. Whisnant, Phys. Lett. B **560**, 75 (2003). [arXiv:hep-ph/0210428](#)
- LBNE Collaboration, C. Adams et al. (2013). [arXiv:1307.7335](#)
- A. Stahl et al. (2012). CERN-SPSC-2012-021, SPSC-EOI-007
- P. Coloma, T. Li, S. Pascoli (2012). [arXiv:1206.4038](#)
- S.K. Agarwalla, T. Li, A. Rubbia, JHEP **1205**, 154 (2012). [arXiv:1109.6526](#)
- M. Blennow et al., JHEP **1307**, 159 (2013). [arXiv:1303.0003](#)
- S.K. Agarwalla, S. Prakash, S. Uma Sankar, JHEP **1403**, 087 (2014). [arXiv:1304.3251](#)
- M. Ghosh et al., JHEP **1403**, 094 (2014). [arXiv:1308.5979](#)
- V. Barger et al., Phys. Rev. D **89**, 011302 (2014). [arXiv:1307.2519](#)
- V. Barger et al. (2014). [arXiv:1405.1054](#)
- D. Dutta, K. Bora, Mod. Phys. Lett. A **30**, 1550017 (2015). [arXiv:1409.8248](#)
- M. Blennow et al., JHEP **1403**, 028 (2014). [arXiv:1311.1822](#)
- M. Blennow, P. Coloma, E. Fernandez-Martinez, JHEP **03**, 005 (2015). [arXiv:1407.3274](#)
- K.N. Deepthi, C. Soumya, R. Mohanta, N. J. Phys. **17**, 023035 (2015). [arXiv:1409.2343](#)
- K. Bora, D. Dutta, P. Ghoshal, Mod. Phys. Lett. A **30**, 1550066 (2015). [arXiv:1405.7482](#)
- LBNE, J. Strait, Talk given at NuFact 2014, August 25–30, 2014, University of Glasgow (2014). <http://www.nufact2014.physics.gla.ac.uk/>
- DUNE, R. Acciarri et al. (2015). [arXiv:1512.06148](#)
- K. Nakamura, Front. Phys. **35**, 359 (2000)
- Hyper-Kamiokande Proto-Collaboration, K. Abe et al., PTEP **2015**, 053C02 (2015). [arXiv:1502.05199](#)
- IceCube-PINGU Collaboration, M. Aartsen et al. (2014). [arXiv:1401.2046](#)
- W. Winter, Phys. Rev. D **88**, 013013 (2013). [arXiv:1305.5539](#)
- S. Choubey, A. Ghosh, JHEP **1311**, 166 (2013). [arXiv:1309.5760](#)
- S.F. Ge, K. Hagiwara, JHEP **09**, 024 (2014). [arXiv:1312.0457](#)
- M. Blennow, T. Schwetz, JHEP **09**, 089 (2013). [arXiv:1306.3988](#)
- E.K. Akhmedov, S. Razaque, A.Yu. Smirnov, JHEP **02**, 082 (2013). [arXiv:1205.7071](#) [Erratum: JHEP **07**, 026 (2013)]
- P. Coloma et al., Phys. Rev. D **87**, 033004 (2013). [arXiv:1209.5973](#)
- P. Huber, J. Kopp, JHEP **1103**, 013 (2011). [arXiv:1010.3706](#)

74. P. Huber, M. Lindner, W. Winter, *Comput. Phys. Commun.* **167**, 195 (2005). [arXiv:hep-ph/0407333](#)
75. P. Huber et al., *Comput. Phys. Commun.* **177**, 432 (2007). [arXiv:hep-ph/0701187](#)
76. M.D. Messier, Ph.D. Thesis (Advisor: James L. Stone) (1999)
77. E. Paschos, J. Yu, *Phys. Rev. D* **65**, 033002 (2002). [arXiv:hep-ph/0107261](#)
78. P. Huber, M. Lindner, W. Winter, *Nucl. Phys. B* **645**, 3 (2002). [arXiv:hep-ph/0204352](#)
79. M. Fechner, Ph.D. Thesis, DAPNIA-2006-01-T
80. T2K Collaboration, I. Kato, *J. Phys. Conf. Ser.* **136**, 022018 (2008)
81. M. Ghosh, S. Goswami, S.K. Raut (2014). [arXiv:1409.5046](#)
82. T2K Collaboration, K. Abe et al. (2014). [arXiv:1409.7469](#)
83. NO ν A, R. Patterson, Talk given at the Neutrino 2012 Conference, June 3–9, 2012, Kyoto (2012). <http://neu2012.kek.jp/>
84. A. Chatterjee et al., *JINST* **9**, P07001 (2014). [arXiv:1405.7243](#)
85. M.M. Devi et al., *JHEP* **1410**, 189 (2014). [arXiv:1406.3689](#)
86. R. Gandhi et al., *Phys. Rev. D* **76**, 073012 (2007). [arXiv:0707.1723](#)
87. LBNE Collaboration, T. Akiri et al. (2011). [arXiv:1110.6249](#)
88. D. Cherdack (2014, Private communication)
89. A. Cervera et al., *Nucl. Phys. B* **579**, 17 (2000). [arXiv:hep-ph/0002108](#)
90. M. Freund, *Phys. Rev. D* **64**, 053003 (2001). [arXiv:hep-ph/0103300](#)
91. E.K. Akhmedov et al., *JHEP* **04**, 078 (2004). [arXiv:hep-ph/0402175](#)
92. H. Nunokawa, S.J. Parke, R. Zukanovich Funchal, *Phys. Rev. D* **72**, 013009 (2005). [arXiv:hep-ph/0503283](#)
93. A. de Gouvea, J. Jenkins, B. Kayser, *Phys. Rev. D* **71**, 113009 (2005). [arXiv:hep-ph/0503079](#)
94. S.K. Raut, *Mod. Phys. Lett. A* **28**, 1350093 (2013). [arXiv:1209.5658](#)
95. Daya Bay, Community Summer Study 2013: Snowmass on the Mississippi (CSS2013) Minneapolis, July 29–August 6 2013 (2013). [arXiv:1309.7961](#)
96. T2K Collaboration, K. Abe et al., *Phys. Rev. D* **87**, 092003 (2013). [arXiv:1302.4908](#)
97. T2K Collaboration, K. Abe et al. (2014). [arXiv:1407.7389](#)
98. MINOS Collaboration, P. Adamson et al. (2014). [arXiv:1410.8613](#)
99. Collaboration A. Kaboth for the T2K, A. Kaboth (2013). [arXiv:1310.6544](#)
100. P. Huber, M. Mezzetto, T. Schwetz, *JHEP* **03**, 021 (2008). [arXiv:0711.2950](#)
101. Indian Institutions and Fermilab Collaboration, B. Choudhary et al., Detailed project report submitted to DAE, India (2012)
102. M.C. Gonzalez-Garcia, M. Maltoni, *Phys. Rev. D* **70**, 033010 (2004). [arXiv:hep-ph/0404085](#)
103. V. Barger et al., *Phys. Rev. D* **76**, 053005 (2007). [arXiv:hep-ph/0703029](#)
104. ESSnuSB Collaboration, E. Baussan et al., *Nucl. Phys. B* **885**, 127 (2014). [arXiv:1309.7022](#)
105. S.K. Agarwalla, S. Choubey, S. Prakash, *JHEP* **1412**, 020 (2014). [arXiv:1406.2219](#)
106. T2K, K. Abe et al., *Phys. Rev. D* **91**, 072010 (2015). [arXiv:1502.01550](#)